J Mater Sci: Mater Electron
DOI 10.1007/s10854-015-3868-4

Capacitive properties of nanocomposite $(FeCoZr)_x(PZT)_{(100-x)}$ produced by sputtering with the use of argon and oxygen ions beam

T. N. Koltunowicz[1] · P. Zukowski[1] · O. Boiko[1] · K. Czarnacka[2] · V. Bondariev[3] · A. Saad[4] · A. V. Larkin[5] · A. K. Fedotov[5]

Received: 9 July 2015 / Accepted: 8 October 2015

Abstract The paper established that, the hopping mechanism of the charge exchange for the $(FeCoZr)_{64.4}(PZT)_{35.6}$ nanocomposite and the additional polarization of tested sample occurs. As frequency increases two frequency areas where capacitance decreases can be observed. Correlation between the conductivity increase and the capacitance decrease has been observed for the both stages of their variability. Voltage resonance phenomenon for the studied material was observed. The zero crossing in the frequency dependence of phase difference transition is accompanied with this phenomenon, which is reflected by a sharp minimum in the capacitance versus frequency characteristics.

1 Introduction

Currently, determination of the properties of the nanosized composite structures is of fundamental importance for the development of nanotechnologies [1, 2]. Nanomaterials are so attractive that their production technologies are systematically enhanced. In-depth recognition of ion technologies and more specifically of the ion-beam sputtering [3–6] or ion implantation [7–9] and of magnetron sputtering [10–12] as well as of the plasma and high-temperature techniques [13–17] makes it possible to produce multi-component nanomaterial structures. From a big amount of chemical methods for the production of thin films it is the sol–gel method and chemical deposition techniques that meet the greatest scientific interest [18–20]. A combination of the liquid and solid components in one material creates a new perspective for investigations into ferrofluids [21, 22] or the moisture content in oil-impregnated cellulose [23, 24]. The mechanical properties of nanocomposites characterized by varied phase composition, significantly differ from the properties of materials of the micro- or millimetre-scale [25–27]. Investigations into quantum phenomena in nanocomposites [28] or the phenomenon of luminescence in semiconductors [29] make possible to determine the charge transport mechanism there. For instance, for the nanocomposite materials of the metal-dielectric type the character of electric conductivity can be determined by the model of the electron transport (hops) between potential wells (nanoparticles of the metallic phase) within the dielectric matrix (hopping conductivity) [30–36].

AC based testing of the electric properties of nanocomposites $(FeCoZr)_{64.4}(PZT)_{35.6}$ has shown that within the frequency range from 5×10^1 Hz to 5×10^6 Hz the electrical conduction is realized by electron tunneling between quantum wells formed by nanoparticles of the metallic phase FeCoZr embedded in a dielectric matrix of PZT [31, 32, 37–39]. Because of the high resistivity of the dielectric material, electric conductivity in the material can be realized only by the hopping charge transport between the metallic nanoparticles. One of the effects of the hopping recharging that has been

✉ T. N. Koltunowicz
t.koltunowicz@pollub.pl

[1] Department of Electrical Devices and High Voltage Technology, Lublin University of Technology, 20-618 Lublin, Poland

[2] Department of Technology Fundamentals, University of Life Sciences in Lublin, 20-612 Lublin, Poland

[3] Sumy State University, 40007 Sumy, Ukraine

[4] Department of Applied Sciences, Al-Balqa Applied University, PO Box 2041, Amman 11953, Salt, Jordan

[5] Belarusian State University, 220030 Minsk, Belarus

Published online: 19 October 2015

observed in nanocomposites is the phenomenon of the coilless-like inductance. It is accompanied with the occurrence of positive phase difference values at alternating current [31, 33, 40] that resemble the phase shift that is characteristic for conventional coils [41]. Another effect of the hopping electron exchange between two neutral potential wells is the formation of dipoles [42]. External electric field induces orientational ordering of the dipoles and thereby leads to an increase of the dielectric permittivity relative to the matrix material [43].

The objective of the presented research project has been to examine experimentally the phenomena of polarization and conductivity occurring in the nanocomposites $(FeCoZr)_{64.4}(PZT)_{35.6}$ produced by the ion-beam sputtering using a combined beam of argon and oxygen ions depending on the AC frequency and the measuring temperature. The mechanism of the elevated dielectric permittivity occurrence in that nanocomposite has been also analyzed.

2 Experiments

The samples of a nanocomposite $(FeCoZr)_x(PZT)_{(100-x)}$ of the metallic phase content ranging from 29 to 90 at.% have been produced using ion-beam sputtering of a target dielectric, composed of the ferromagnetic alloy FeCoZr and strips of the PZT, as has been described in [39, 44, 45]. The sputtering has been realized with a combined beam of argon ions of the pressure of $P_{Ar} = 7.4 \times 10^{-2}$ Pa and the oxygen ions of the pressure of $P_{O2} = 3 \times 10^{-3}$ Pa. The paper presents measurement results obtained for a nanocomposite of the metallic phase content of $x = 64.4$ at.%.

The chemical composition has been determined with the application of scanning electron microscopy (SEM, LEO 1455VP) and X-ray microanalysis (EDX). The contents of individual elements have been determined with the accuracy of ~ 1 at.%.

Measurements of frequency and temperature dependences of the conductivity $\sigma(f, T_p)$, phase difference $\theta(f, T_p)$, capacitance $C_p(f, T_p)$ and loss coefficient $\tan\delta(f, T_p)$ have been performed using a laboratory setup for AC-based testing electric properties [46] designed and built in the Department of Electrical Devices and High Voltage Technology of the Lublin University of Technology. The obtained samples have been tested using alternating current within the frequency range of 50–5 MHz using measuring temperatures of $T_p = 77$–373 K at the temperature change step of 5 K. Each completed measuring cycle has been followed by 15-min annealing of a sample in a tubular furnace in air using temperatures T_a ranging from 398 to 798 K at the temperature change step of 25 K.

3 Experimental results and their analysis

Figure 1 presents selected capacitance versus frequency dependences for a sample of the nanocomposite $(FeCoZr)_x(PZT)_{(100-x)}$ of the metallic phase content $x = 64.4$ at.%, subdued to 15-min annealing in the temperature of 498 K.

Figure 1 shows that within the frequency range from 50 Hz to ca 10^3 Hz the capacitance practically does not depend on the measuring frequency. Within that frequency range, along with the temperature growth from 81 to 218 K an insignificant capacitance increase by about 1.6 times can be observed for the frequency of 10^2 Hz. As the frequency reaches values exceeding 10^3 Hz, a rapid capacitance decrease by ca 20 times occurs followed by a considerable reduction of the decrease rate up to the moment, when the capacitance gets almost constant at the frequency value of 3×10^4 Hz. Further frequency increase up to above 5×10^4 Hz leads to the occurrence of the second stage of the capacitance decrease. At the frequency value of ca 1.5×10^6 Hz, a sharp minimum of the capacitance value occurs. A comparative analysis of the frequency dependences of the capacitance (Fig. 1) and the phase difference (Fig. 2) indicates that the minimum observed in the capacitance versus frequency characteristic perfectly coincides with the frequency value, when $\theta = 0°$ i.e. when the voltage resonance occurs in the conventional series RLC circuits [31, 32].

Figure 3 presents the capacitance versus frequency characteristic, while Fig. 4 shows the frequency dependence of conductivity. Linear scale has been chosen for

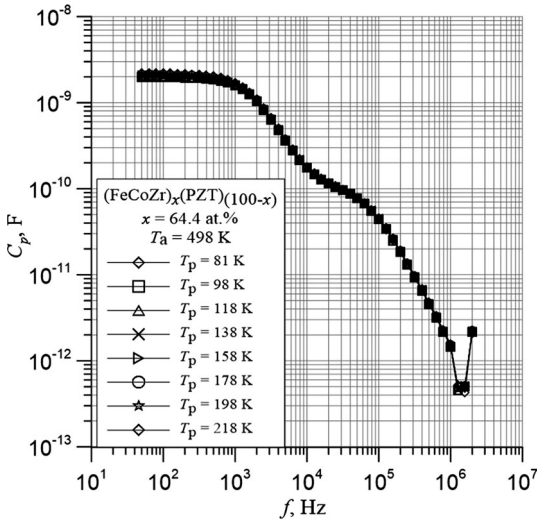

Fig. 1 Capacitance versus frequency dependence obtained for a nanocomposite sample of $(FeCoZr)_x(PZT)_{(100-x)}$ of the metallic phase content $x = 64.4$ at.%, subdued to 15-min annealing in the temperature of 498 K for selected measuring temperatures of T_p

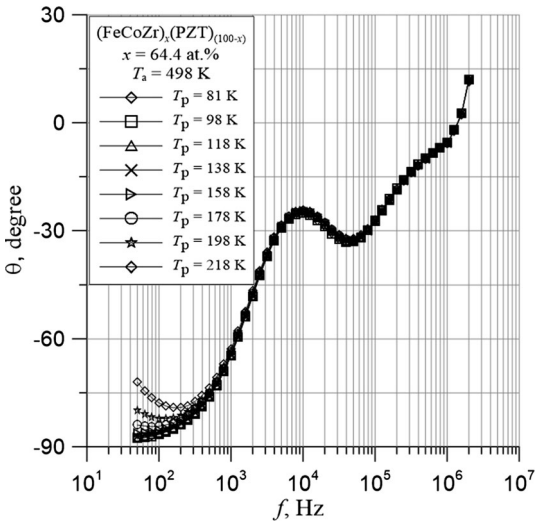

Fig. 2 Phase difference versus frequency dependence obtained for the nanocomposite $Z(FeCoZr)_x(PZT)_{(100-x)}$ of the metallic phase content $x = 64.4$ at.%, subdued to 15-min annealing in the temperature of 498 K for selected measuring temperatures of T_p

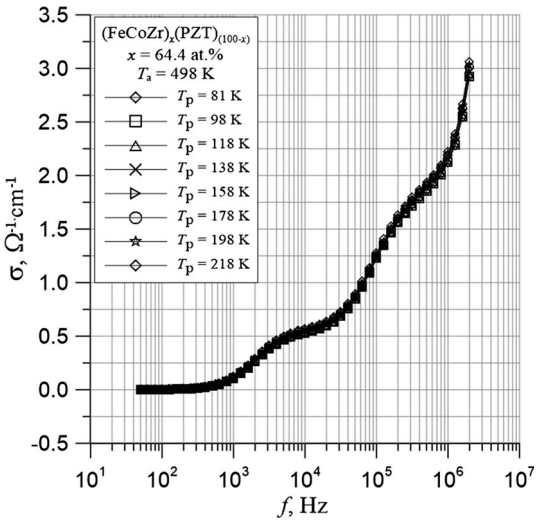

Fig. 4 Conductivity versus frequency dependence obtained for a sample of the nanocomposite $(FeCoZr)_x(PZT)_{(100-x)}$ of the metallic phase content $x = 64.4$ at.%, subdued to 15-min annealing in the temperature of 498 K for selected measuring temperatures of T_p

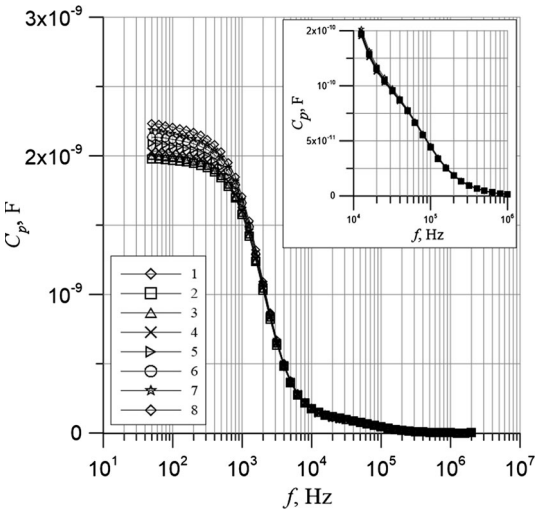

Fig. 3 Capacitance versus frequency dependence obtained for a nanocomposite sample of $(FeCoZr)_x(PZT)_{(100-x)}$ of the metallic phase content $x = 64.4$ at.%, subdued to 15-min annealing in the temperature of 498 K. for selected measuring temperatures of T_p

their presentation in order to determine mean values of the permittivity and conductivity relaxation times. It is known [47] that for the angular frequency:

$$\omega = 2\pi f = 1/\tau \quad (1)$$

the dielectric permittivity value doubly decreases and the conductivity value is twofold lower than its steady state value at higher frequency values. It means that the analysis of changes in the frequency dependences shown in Figs. 3 and 4 makes it possible to easily determine mean values of time constants for the both variation stages of the permittivity and conductivity. Mean values of the permittivity relaxation time can be determined using the plot of Fig. 3 and marking the points, where the permittivity is equal to half of the difference of the flat segments for the both variation stages (before and after rapid increasing segment). Mean values of the conductivity relaxation time can be determined by applying a similar procedure to the characteristic shown in Fig. 4. Figures 3 and 4 show that for both the permittivity and the conductivity the mean relaxation time value is of ca 8×10^{-5} s for the first variation stage and of ca 3×10^{-7} s for the other stage. It means that in the tested nanocomposite $(FeCoZr)_x(PZT)_{(100-x)}$ there is a correlation between the conductivity increase and the decrease of capacitance for the both stages of their variations.

In order to determine activation energy values, Arrhenius graphs have been plotted for the permittivity (Fig. 5) and the conductivity (Fig. 6) for measuring frequencies of 100 Hz (the first stage) and of 20 kHz (the second stage).

The activation energy values that have been determined based on those plots in the case of permittivity are of $\Delta E_{C1} \approx 3.23$ meV for the frequency of 100 Hz (preceding the first decrease stage) and of $\Delta E_{C2} \approx 0.73$ meV for the frequency of 20 kHz (in between of the two decrease stages). In the case of conductivity for the frequency of 100 Hz (preceding the first increase stage) the energy activation value is of $\Delta E_{\sigma 1} \approx 91.4$ meV, while for the frequency of 20 kHz, that is between the first and the second increase stage, the value amounts to $\Delta E_{\sigma 2} \approx 2.27$ meV.

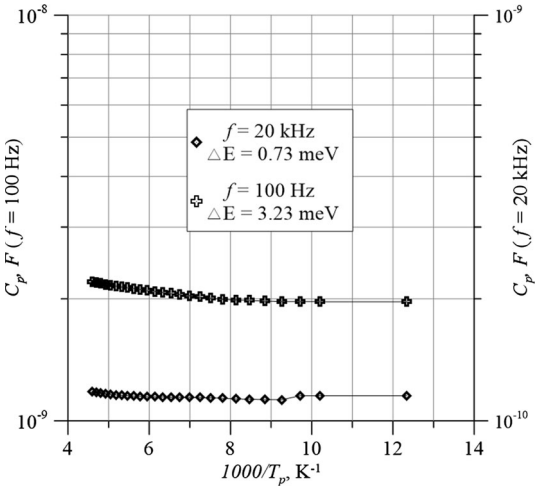

Fig. 5 Arrhenius plot for the capacitance of a nanocomposite sample of $(FeCoZr)_x(PZT)_{(100-x)}$ of the metallic phase content x = 64.4 at.%, subdued to 15-min annealing in the temperature of 498 K for the frequency values of 100 Hz (scale at the *left side*) and of 20 kHz (scale at the *right side*)

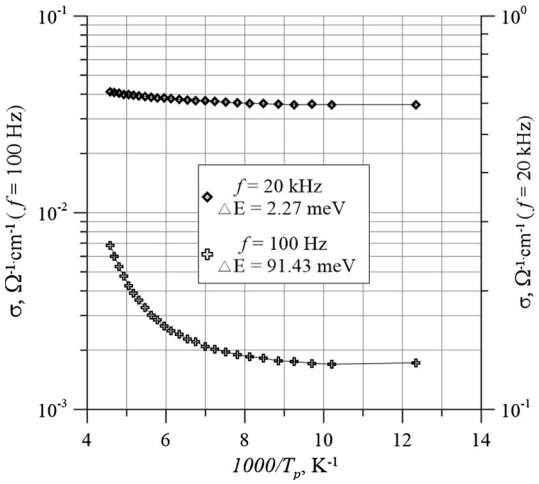

Fig. 6 Arrhenius plot for the conductivity of a nanocomposite sample of $(FeCoZr)_x(PZT)_{(100-x)}$ of the metallic phase content x = 64.4 at.%, subdued to 15-min annealing in the temperature of 498 K for the frequency values of 100 Hz (scale at the *left side*) and of 20 kHz (scale at the *right side*)

When a nanocomposite contains a high concentration of potential wells, distances between them reach down to several dozen nanometers or less and favorable conditions for the electron tunneling between the wells occur. Electric current conduction that is related to that phenomenon is referred as hopping conductivity. It has been experimentally established [42] that the hopping exchange of electrons between the neutral potential wells brings about the formation of dipoles and consequently an additional polarization of the material that can be described by the below given formula derived in [43]:

$$\varepsilon_P = 1 + \frac{N \cdot P(T) \cdot \tau \cdot e^2 \cdot R^2}{\varepsilon_0 \cdot k \cdot T} \tag{2}$$

where $P(T)$—probability of hops per a time unit, N—concentration of potential wells; τ—relaxation time—time lapse between an electron hop from one neutral potential well to another and its return back to the initial well: e—elementary charge; R—mean hop length; ε_0—vacuum permittivity, k—Boltzmann constant; T—temperature.

Following [48–50], the probability of hops per a time unit $P(T)$ of the formula (1) can be written in the following generalized form:

$$P(T) = P_0 \cdot \exp\left(-2 \cdot \alpha \cdot R - \frac{\Delta E_t}{k \cdot T}\right) \tag{3}$$

where P_0—numerical coefficient weakly dependent on the mean hop length R and the temperature T; ΔE_t—activation energy of electron hops; α—inverse value of the hopping electron localization radius in a potential well.

The expression:

$$\exp(-2 \cdot \alpha \cdot R) \tag{4}$$

describes the collapse rate of the hopping electron wave function outside the potential well.

By substituting the value of $P(T)$ of the formula (3) to the permittivity formula (2) the below given formula for static electric permittivity can be obtained:

$$\varepsilon_P = 1 + P_0 \frac{N \cdot \tau \cdot e^2 \cdot R^2}{\varepsilon_0 \cdot k \cdot T} \exp\left(-2 \cdot \alpha \cdot R - \frac{\Delta E_t}{k \cdot T}\right) \tag{5}$$

It follows from (5) that in the low AC frequency area the dielectric permittivity of a material that contains dense concentration of potential wells is not frequency dependent. When angular frequency ω approaches $1/\tau$, the permittivity value begins to decrease and tends towards a value that is characteristic for a material that does not contain potential wells.

The relaxation time that can be found in the formulas (2) and (5) is exponentially temperature dependent [51, 52]:

$$\tau(T) = \tau_0 \cdot \exp\left(\frac{\Delta E_\tau}{k \cdot T}\right) \tag{6}$$

where τ_0—numerical coefficient; ΔE_τ—activation energy of the relaxation time.

Relaxation time is a function of the distance that a hopping electron should cover [53]. Distances between individual nanoparticles are random values and that is why probability distribution of the relaxation time values occurs in the nanocomposites. That probability distribution can be described using e.g. the Moyal approximation of the Landau distribution [54].

By substituting the relaxation time value of (6) to the formula (5) the following can be obtained:

$$\varepsilon_P = 1 + P_0 \cdot \tau_0 \frac{N \cdot e^2 \cdot R^2}{\varepsilon_0 \cdot k \cdot T} \exp\left(-2 \cdot \alpha \cdot R - \frac{\Delta E_t - \Delta E_\tau}{k \cdot T}\right) \quad (7)$$

In the low frequency area, the direct current (low frequency) conductivity can be written in the following form [50]:

$$\sigma(T) = \sigma_0 \cdot \exp\left(-2 \cdot \alpha \cdot R - \frac{\Delta E_t}{k \cdot T}\right) \quad (8)$$

Comparative analysis of the formulas for the static dielectric permittivity (7) and for the direct current conductivity (8) indicates that the conductivity activation energy should be higher than the static permittivity activation energy, because:

$$\Delta E_t - \Delta E_\tau = \Delta E_C < \Delta E_t = \Delta E_\sigma \quad (9)$$

A comparison of activation energy values for the static dielectric permittivity of $\Delta E_{C1} \approx 3.23$ meV (Fig. 5) and for the low-frequency conductivity of $\Delta E_{\sigma 1} \approx 91.4$ meV (Fig. 6) proves validity of the inequality (9) that is based on the model of conductivity and polarization at direct and alternating current [31, 55].

4 Conclusions

The temperature and frequency dependences of the capacity, conductivity and phase difference transition have been tested for a $(FeCoZr)_x(PZT)_{(100-x)}$ nanocomposite of metallic phase content x = 64.4 at.%. The nanocomposite film was followed by a 15-min annealing process in the air in temperature of 498 K. Three frequency areas, where capacity practically does not depend on frequency, and two frequency areas, where capacity decrease, are observed for the frequency range of 50–5 MHz. According to the frequency grows direction the order of these areas is located as follows: the first weekly depended stage (almost constant); the first decreasing stage characterized by the relaxation time value of τ_1 8 × 10^{-5} s; the second weekly depended stage; the second decreasing stage characterized by the relaxation time value of τ_2 3 × 10^{-7} s; the third weekly depended stage. In contrast, the frequency dependence of conductivity looks like a mirror image relative to the horizontal axis: the first weekly depended stage; the first increasing stage; the second weekly depended stage; the second increasing stage; the third weekly depended stage. Frequency dependences of capacity and conductivity indicate a hopping mechanism of the charge exchange between the metallic phase nanoparticles. In the frequency area of above 1 MHz, the phase difference transition from negative values (typical for the capacitive type of conduction) through zero to positive vales (typical for the inductive type of conduction) occurs. The voltage resonance phenomenon can be observed for the nanocomposite film. Based on the Arrhenius plots, activation energy values have been determined for the capacitance and conductivity of a nanocomposite $(FeCoZr)_{64.4}(PZT)_{35.6}$ for the both stages of their variations.

Acknowledgments This research was partially funded from: the statute tasks of the Lublin University of Technology, at the Faculty of Electrical Engineering and Computer Science, S-28/E/2015, entitled 'Preparation of nanolayers and nanocomposites metal or semiconductor in the dielectric matrix and the study of their electrical and magnetic properties'; the statute grant for Ph.D. students at the Faculty of Electrical Engineering and Computer Science; the research project No. IP 2012 026572 within the Iuventus Plus program of the Polish Ministry of Science and Higher Education in the years 2013–2015.

References

1. A.D. Pogrebnjak, A.P. Shpak, N.A. Azarenkov, V.M. Beresnev, Usp Fiz Nauk+. **179**(1), 35 (2009)
2. A.D. Pogrebnjak, V.M. Beresnev, *Nanocoatings Nanosystems Nanotechnologies* (Bentham Science, Oak Park, 2012)
3. F.F. Komarov, L.A. Vlasukova, O.V. Milchanin, M. Makhavikou, I. Parkhomenko, E. Wendler, W. Wesch, G. Ismailova, M. Opielak, Thin Films of SiO_2 Ion-Implanted with Sn: Evaluation of Structure and Composition. In: Grigonis A (ed), *5th International Conference Radiation Interaction with Materials: Fundamentals and Applications* (2014), pp. 385–388
4. O.V. Dunets, Y.E. Kalinin, M.A. Kashirin, A.V. Sitnikov, Tech. Phys. **58**(9), 1352 (2013)
5. A.V. Ivanov, Y.E. Kalinin, V.N. Nechaev, A.V. Sitnikov, Phys. Solid State **51**(12), 2474 (2009)
6. O.V. Stognei, A.V. Sitnikov, Anisotropy of amorphous nanogranular composites CoNbTa–SiO_n and CoFeB–SiO_n. Phys. Solid State **52**(12), 2518 (2010)
7. V.N. Popok, V.I. Nuzhdin, V.F. Valeev, A.L. Stepanov, J. Mater. Res. **30**(1), 86 (2015)
8. L. Himics, S. Toth, M. Veres, A. Toth, M. Koos, Appl. Surf. Sci. **328**, 577 (2015)
9. M.C. Salvadori, F.S. Teixeira, L.G. Sgubin, M. Cattani, I.G. Brown, Appl. Surf. Sci. **310**, 158 (2014)
10. F.F. Komarov, S.V. Konstantinov, V.V. Pilko, J. Frict. Wear **35**(3), 215 (2014)
11. C.A. Kumar, D. Pamu, Appl. Surf. Sci. **340**, 56 (2015)
12. M. Mazur, D. Kaczmarek, E. Prociow, J. Domaradzki, D. Wojcieszak, J. Bochenski, Mater. Sci. Pol. **32**(3), 457 (2014)
13. A.V. Lozhechnik, A.L. Mosse, High Temp. Mater. Processes (NY) **16**(2), 81 (2012)
14. H. Sari, V.M. Astashynski, E.A. Kostyukevich, A.M. Kuzmitski, V.V. Uglov, N.N. Cherenda, YuA Petukhou, High Temp. Mater. Processes (NY) **16**(4), 297 (2012)
15. Chun-Liang Yeh, Guan-Shiung Teng, High Temp. Mater. Processes (NY) **16**(1), 45 (2012)

16. S.N. Bratushka, M. Opielak, S. Liscak, Prz. Elektrotech. **88**(10A), 314 (2012)
17. A.D. Pogrebnjak, G. Abadias, O.V. Bondar, B.O. Postolnyi, M.O. Lisovenko, O.V. Kyrychenko, A.A. Andreev, V.M. Beresnev, D.A. Kolesnikov, M. Opielak, Acta Phys. Pol. A **125**(6), 1280 (2014)
18. Y. Zhang, X.H. Zhu, S.H. Zhou, J.M. Zhu, Z.G. Liu, T. Al-Kassab, J. Nanopart. Res. **16**(1), 2208 (2013)
19. G.A.M. Ali, O.A. Fouad, S.A. Makhlouf, J. Alloys Compd. **579**, 606 (2013)
20. K.G. Gareev, I.E. Gracheva, V.A. Moshnikov, Glass Phys. Chem. **39**(5), 548 (2013)
21. J. Kudelcik, P. Bury, P. Kopcansky, M. Timko, J. Magn. Magn. Mater. **388**, 28 (2015)
22. J. Kúdelčík, P. Bury, J. Drga, P. Kopčanský, V. Závišová, M. Timko, Acta Phys. Pol. A **121**(5–6), 1169 (2012)
23. P. Żukowski, T.N. Kołtunowicz, K. Kierczyński, J. Subocz, M. Szrot, M. Gutten, IEEE Trans. Dielectr. Electr. Insul. **21**(3), 1268 (2014)
24. P. Zukowski, T.N. Kołtunowicz, K. Kierczynski, J. Subocz, M. Szrot, Cellulose **22**, 861 (2015)
25. A.D. Pogrebnjak, J. Nanomater. Article number 780125 (2013)
26. P. Misaelides, A. Hatzidimitriou, F. Noli, A.D. Pogrebnjak, Y.N. Tyurin, S. Kosionidis, Surf. Coat. Technol. **180**, 290 (2004)
27. F. Noli, P. Misaelides, A. Hatzidimitriou, E. Pavlidou, A.D. Pogrebnjak, Appl. Surf. Sci. **252**(23), 8043 (2006)
28. Y. Imry, *Introduction to Mesoscopic Physics* (University Press, Oxford, 2002)
29. J. Zuk, R. Kuduk, M. Kulik, J. Liskiewicz, D. Maczka, P.V. Zhukovski, V.F. Stelmakh, V.P. Bondarenko, A.M. Dorofeev, J. Lumin. **57**(1–6), 57 (1993)
30. T.N. Koltunowicz, J. Mater. Sci. Mater. Electron. **26**(9), 6450 (2015)
31. T.N. Kołtunowicz, J.A. Fedotova, P. Zhukowski, A. Saad, A. Fedotov, J.V. Kasiuk, A.V. Larkin, J. Phys. D Appl. Phys. **46**(12), 125304 (2013)
32. T.N. Kołtunowicz, P. Zhukowski, A.K. Fedotov, A.V. Larkin, A. Patryn, B. Andriyevsky, A. Saad, J.A. Fedotova, V.V. Fedotova, Elektronika ir Elektrotechnika (Electron. Electr. Eng.) **19**, 437 (2013)
33. P. Zhukowski, T.N. Kołtunowicz, P. Węgierek, J.A. Fedotova, A.K. Fedotov, A.V. Larkin, Acta Phys. Pol. A **120**(1), 43 (2011)
34. M. Ershov, H.C. Liu, L. Li, M. Buchanan, Z.R. Wasilewski, A. Jonscher, IEEE Trans. Electron Devices **45**(10), 2196 (1998)
35. H.L. Kwok, Solid State Electron. **47**(6), 1089 (2003)
36. L. Bakueva, G. Konstantatos, S. Musikhin, H.E. Ruda, A. Shika, Appl. Phys. Lett. **85**(16), 3567 (2004)
37. T.N. Koltunowicz, P. Zukowski, O. Boiko, A. Saad, J.A. Fedotova, A.K. Fedotov, A. Larkin, J. Kasiuk, J. Electron. Mater. **44**(7), 2260 (2015)
38. T.N. Koltunowicz, Acta Phys. Pol. A **125**(6), 1412 (2014)
39. A.V. Larkin, A.K. Fedotov, J.A. Fedotova, T.N. Koltunowicz, P. Zhukowski, Mater. Sci. Pol. **30**(2), 75 (2012)
40. T.N. Kołtunowicz, P. Żukowski, V. Bondariev, J.A. Fedotova, A.K. Fedotov, Vacuum 120 (Part B), 44 (2015)
41. D. Halliday, R. Resnick Physics, Part II, (John Wiley & Sons, New York, 1978)
42. P.W. Zukowski, S.B. Kantorow, K. Kiszczak, D. Maczka, V.F. Stelmakh, A. Rodzik, E. Czarnecka-Such, Phys. Status Solidi A Appl. Res. **128**(2), K117 (1991)
43. P.W. Zukowski, A. Rodzik, Y.A. Shostak, Semiconductors **31**(6), 610 (1997)
44. YuE Kalinin, A.T. Ponomarenko, A.V. Sitnikov, O.V. Stogney, Phys. Chem. Mater. Treat. **5**, 14 (2001)
45. I.V. Zolotukhin, YuE Kalinin, A.T. Ponomarenko, V.G. Shevchenko, A.V. Sitnikov, O.V. Stognei, O. Figovsky, J. Nanostruct. Polym. Nanocompos. **2**, 23 (2006)
46. F.F. Komarov, P. Zhukowski, R.M. Krivosheev, E. Munoz, T.N. Koltunowicz, V.N. Rodionova, A.K. Togambaeva, Phys. Status Solidi A Appl. Mater. Sci. **212**(2), 425 (2015)
47. A.K. Jonscher, *Dielectric Relaxation in Solids* (Chelsea Dielectrics Press, London, 1983)
48. N.F. Mott, E.A. Davis, *Electron Processes in Non-crystalline Materials* (Claredon Press, Oxford, 1979)
49. S.S. Kirkpatrik, in *Proceedings of the 5th International Conference on Amorphous and Liquid Semiconductors*, (Garmish-Partenkirchen, 1973), pp.183–190
50. B.I. Shklovsky, A.L. Efros, *Elecronic Properties of Doped Semiconductors* (Springer, Berlin, 1984)
51. G.C. Psarras, E. Manolakaki, G.M. Tsangaris, Compos. A Appl. Sci. Manuf. **34**(12), 1187 (2003)
52. M.A. Kudryashov, A.I. Mashin, A.A. Logunov, G. Chidichimo, G. De Filpo, Tech. Phys. **57**(7), 965–970 (2012)
53. P.V. Zukowski, J. Partyka, P. Wegierek, J.W. Sidorenko, J.A. Szostak, A. Rodzik, Semiconductors **33**(3), 276 (1999)
54. J.E. Moyal, Philos. Mag. **46**, 263 (1955)
55. T.N. Kołtunowicz, P. Żukowski, O. Boiko, V. Bondariev, K. Czarnacka, J.A. Fedotova, A.K. Fedotov, I.A. Svito, Vacuum 120 (Part B), 37 (2015)